Investigation of the controlled bond expansion time-dependent variational principle for open quantum systems

Guided Research

Jeremiah Bintang Santoso

Supervised by Prof. Dr. Christian Mendl

Chair of Scientific Computing in Computer Science

Advised by Richard Milbradt, M.Sc

Abstract

In this guided research report, I present the results of investigating the new time-dependent variational principle method with controlled bond expansion to time-evolve open quantum systems, specifically the spin-boson model. The model was first formulated in the hierarchy of matrix product states before time-evolving it. The results are compared with the two-site version results because it has a higher accuracy than the one-site version, from which the controlled bond expansion version is based. The results prove that the controlled bond expansion version can expand and grow its bond dimensions while still having the running time of the one-site version in an open quantum system setting. Although the accuracy changes depending on the complexity of the model, the method can still get the two-site results by tweaking its hyperparameters and enabling an additional orthogonalization process. The method holds much promise and it should be tested in more complex scenarios.

1. Introduction

Studying open quantum systems is an interesting topic because it describes a lot of the phenomena that we have seen in nature like the photosynthesis process and also in emerging technology like quantum computers [1, 2]. However, it is not an easy task as the coupling between the system in observation and the noise from the environment makes it hard to analyze and compute. The tensor networks method has been a blessing to the research field as it gives researchers the ability to model the relationship between the quantum states in a simple and easily understandable manner while unlocking a lot of existing and powerful methods from linear algebra [3]. One type of widely used tensor network is the matrix product state (MPS) also called a tensor train (TT).

The way the system transmits information in an MPS is through the bonds between the tensors, specifically the size of the bond dimension indicates how much information is being transmitted. As such, it is crucial to have a method to time-evolve a quantum system that gives an accurate increase or decrease of the dimension in an efficient manner. One way to do it is called the time-dependent variational principle (TDVP) [4]. It is a general method given an MPS with its corresponding Hamiltonian. So, as long as we can formulate an open quantum system as an MPS, we can time-evolve it with TDVP.

When an open quantum system is presented in the non-Markovian quantum state diffusion (NMQSD) equation, like in simulating absorption spectra of molecular aggregates, the current standard to simulate it is the hierarchy of pure states (HOPS) method [5, 6]. HOPS is powerful because it is a formally exact method to efficiently solve NMQSD equations. There have been some developments to integrate HOPS and MPS, resulting in a method called the hierarchy of matrix product states (HOMPS) [7].

In this guided research, I implemented a new method called the controlled bond expansion (CBE) TDVP by Li et al. [8] for open quantum systems. [8] claims the method to have the efficiency of the one-site TDVP (TDVP1) with the accuracy of the two-site TDVP (TDVP2). I then compared the performance and results from CBE-TDVP with the ones from TDVP2 in the model case of the transverse-field Ising model and the spin-boson model, some of the trademark cases of quantum systems.

In Section 2, I will discuss the TDVP method briefly and continue with the discussion of the toy model in Section 3. The actual implementations are discussed in Section 4 and the results are shown in Section 5. Finally, I close this report with a conclusion and suggestions for further research in Section 6.

2. Time-dependent variational principle (TDVP)

The main goal of TDVP is to time-evolve the MPS while constraining it to the manifold generated by the MPS given the initial bond dimension. The manifold can be seen as the solution space of the MPS. To do this, we project the right-hand side of the Schrödinger equation onto the tangent space. The time-dependent Schrödinger equation becomes

$$\frac{\partial |\Psi\rangle}{\partial t} = -i\hat{P}_{T|\Psi\rangle}\hat{H}|\Psi\rangle \tag{1}$$

where $\hat{P}_{T|\Psi\rangle}$ is the projector to the tangent space of the MPS.

The most common variants of TDVP are TDVP1 and TDVP2 [9]. The main difference of interest between these methods is that TDVP1 can only have fixed bond dimensions during the evolution while TDVP2 can increase or decrease the dimensions accordingly. The flexibility of the bond dimensions is crucial because this enables TDVP2 to simulate the system more accurately. However, as with other great methods, TDVP2 needs significantly more compute time than TDVP1.

In 2022, [8] implemented a method which allows TDVP1 to grow its bond dimensions at a certain rate. This method is what we call the CBE-TDVP method. The method is an extension of an idea the group has implemented to the density matrix renormalization group (DMRG) algorithm [10].

Given an MPS in Figure 1, during the right-to-left sweep in updating tensor A_l, we want to expand the bond dimensions of A_{l-1} to $A_{l-1} \oplus \tilde{A}^{tr}_{l-1}$ where $\tilde{A}^{tr}_{l-1}$ is obtained from a truncated $\overline{A}_{l-1}$. This expansion is done using an algorithm called the shrewd selection. There are two truncation processes: the first one is called the preselection and it produces the tensor $\hat{A}^{pr}_{l-1}$ from $\overline{A}_{l-1}$; the second one is called the final selection and it produces the tensor $\tilde{A}^{tr}_{l-1}$ from $\hat{A}^{pr}_{l-1}$. The algorithm is available in the Supplemental Material of [10].

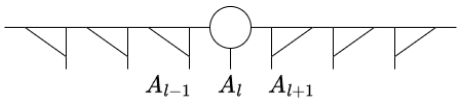

Figure 1: MPS model

The shrewd selection process has a health check which checks the orthogonality of the candidate $\hat{A}^{pr}_{l-1}$ that we define as $\hat{U}$ with the original tensor A_{l-1}, i.e. $A^{\dagger}_{l-1}\hat{U} \stackrel{!}{=} 0$. There is an optional step to ensure this condition by adding an additional orthogonalization where we do an SVD on $\hat{U} - A_l A^{\dagger}_l \hat{U}$ to get the $\hat{U}^{new}$. We then use $\hat{U}^{new}$ as $\hat{A}^{pr}_{l-1}$.

3. Toy model

I used two toy models for different experiments. The first model is the transverse-field Ising (TFI) model just for its simplicity and to check the speed between different methods. One of the other reasons is that the current implementation of TDVP1 couldn't be used for other complicated models. The Hamiltonian of the TFI model is as follows

$$\hat{H} = -J \sum_{i}^{L} \hat{\sigma}_i^x \hat{\sigma}_{i+1}^x - g \sum_{i}^{N} \hat{\sigma}_i^z \tag{2}$$

where J and g are the coupling parameters and $\hat{\sigma}_i^x$ and $\hat{\sigma}_i^z$ are the Pauli X and Z matrices of site i.

For the second model, I used the spin-boson (SB) model. The model describes a simple two-level quantum system interacting with its environment. The system is described as a spin-1/2 particle like a qubit and the environment is modelled as the collection of harmonic oscillators called the bosonic bath. The total Hamiltonian can be written in the typical Hamiltonian for an open system

$$\hat{H} = \hat{H}_S + \hat{H}_B + \hat{H}_{int} \tag{3}$$

where $\hat{H}_S$, $\hat{H}_B$, $\hat{H}_{int}$ are the system, bath, and interaction Hamiltonians respectively. The system Hamiltonian is

$$\hat{H}_S = -\frac{1}{2}\Delta\hat{\sigma}_x + \frac{1}{2}\epsilon\hat{\sigma}_z \tag{4}$$

with $\hat{\sigma}_x$ and $\hat{\sigma}_z$ are Pauli X and Z matrices respectively while Δ and ϵ are coefficients. The bath Hamiltonian is

$$\hat{H}_B = \sum_{k=1}^{K} \nu_k \hat{a}_k^\dagger \hat{a}_k \tag{5}$$

where $\hat{a}_k^\dagger$ and $\hat{a}_k$ are the creation and annihilation operators respectively of the k-th bath mode with ν_k is the corresponding coefficient. Lastly, the interaction Hamiltonian is

$$\hat{H}_{int} = \sum_{k=1}^{K} \gamma_k^* (\hat{L} \otimes \hat{a}_k^\dagger + \text{h.c.}) \tag{6}$$

where $\hat{L}$ operator describes the coupling between the system with the bath modes with γ_k^* describing the strength of the coupling and h.c. refers to the Hermitian complement of $\hat{L} \otimes \hat{a}_k^\dagger$.

In the next section, I will discuss the implementations of these equations.

4. Implementation

The TFI model is simulated with the parameters in Table 1. All TDVP methods share the same parameters except D_{max} and $\tilde{D}$ which are specifically for CBE-TDVP. This is also applicable to the SB model.

Table 1: Parameters of the TFI model

Parameter	Value
Number of sites L	14
Coupling strength J	1
Coupling strength g	1.5
SVD's truncation threshold ϵ	10^{-10}
Maximum bond dimension D_{max}	20
Truncated complement dimension $\tilde{D}$	2
Health check threshold	10^{-10}

For the SB model, it is first converted to the NMQSD equation as follows

$$\frac{\partial \left|\Psi_t\right\rangle}{\partial t} = -i\hat{H}_S \left|\Psi_t\right\rangle + \hat{L} z_t^* \left|\Psi_t\right\rangle - \hat{L}^\dagger \int_0^t ds \alpha(t-s) \frac{\delta \left|\Psi_t\right\rangle}{\delta z_s^*} \tag{7}$$

where α is called the bath correlation function which characterizes the influence of the environment on the system and z_s^* is the noise. HOPS is then used to solve the NMQSD equation and more specifically the non-linear HOPS method

$$\frac{\partial \left|\Psi_t^{(n)}\right\rangle}{\partial t} = (-i\hat{H}_S - \boldsymbol{n}\cdot\boldsymbol{\omega} + \hat{L} z_t^*) \left|\Psi_t^{(n)}\right\rangle + \hat{L} \sum_{k=1}^{K} n_k g_k \left|\Psi_t^{(n-e_k)}\right\rangle - (\hat{L}^\dagger - \langle \hat{L}^\dagger \rangle) \sum_{k=1}^{K} \left|\Psi_t^{(n+e_k)}\right\rangle \tag{8}$$

where z_t^* can be 0 to result in a noise-free HOPS [5].

This non-linear HOPS equation is then time-evolved with the TDVP methods by first adapting the quantum states to MPS form, giving us the HOMPS version. I will not be discussing the whole derivations and explanations of the equations in this report as it has been done in the Bachelor's Thesis of B. Sappler [11].

Table 2 shows the parameters used for the SB simulations.

The important hyperparameters to note for CBE-TDVP are D_{max} and $\tilde{D}$. The first parameter acts as a limit that when the dimensions have reached D_{max}, shrewd selection is disabled. The second parameter essentially represents the additional dimension to add during the sweep.

Table 2: Parameters of the SB model. The values inside the square brackets, e.g. [x/y/z], are options used in the simulations. The first values are the default options if not stated otherwise.

Parameter	Value
Number of sites L	1 system site and 4 bath sites
Coupling strength w	$0.5 + i2$
Coupling strength g	[$0.01/0.1/1/10/100$]
SVD's truncation threshold ϵ	[$10^{-10}/10^{-5}/10^{-13}/10^{-14}/10^{-15}$]
Maximum bond dimension $D_{\max}$	20
Truncated complement dimension $\tilde{D}$	1
Health check threshold	10^{-10}
Noise z_t^*	[True / False]
Additional orthogonalization	[False / True]

As for the health checks threshold, it is to trigger the additional orthogonalization if the step is enabled.

Before moving on to the results and analysis, I need to make one remark about the simulations. Because I didn't have the analytical solutions for these models and problems, I used TDVP2 as the benchmark. So it is assumed that TDVP2 results are the correct solutions and the other methods are assessed by the TDVP2 results. Now, we will discuss the results in the next section.

5. Results

First, I am going to discuss the results of the TFI model. Figure 2 and Table 3 show the simulation results with TDVP1, TDVP2, and CBE-TDVP using the parameters from Table 1. It is good news that the calculated magnetizations are almost identical. This simple simulation proves that the CBE-TDVP works as it can produce the same result as TDVP1 and TDVP2 while growing its bond dimensions. Additionally, it also proves that in this specific case, the running time of CBE-TDVP is practically the same as TDVP1, saving 69% of the TDVP2 running time.

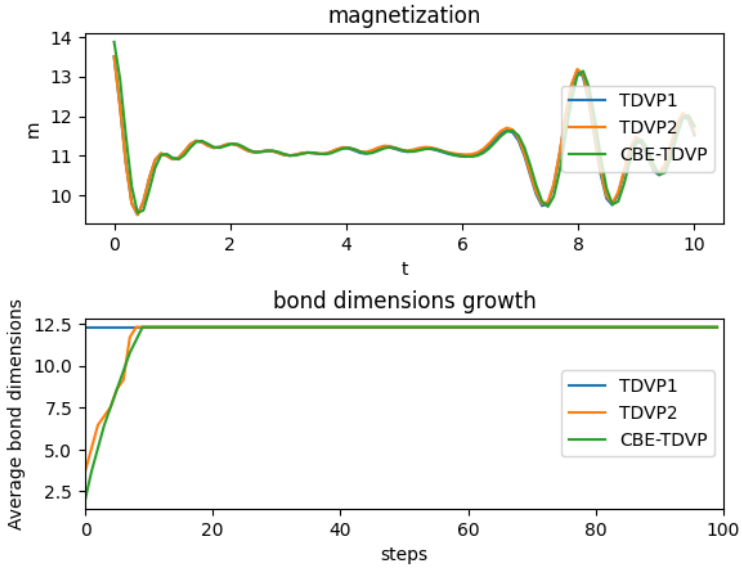

Figure 2: Results from Table 1 for the TFI model using different TDVP methods

Table 3: Running time for the TDVP methods for the TFI model

Method	Running time (s)	Average bond dimensions at steady-state
CBE-TDVP	67.25	12.3
TDVP1	67.12	12.3
TDVP2	213.56	12.3

We can see further interesting behaviour of CBE-TDVP in the SB model simulations. Table 4 shows the results from the model with $g \in \{0.01, 0.1, 1, 10, 100\}$.

The first obvious observation is that CBE-TDVP is still faster than TDVP2. Interestingly, the difference between these two methods is more apparent when the computations are more demanding. When TDVP2 fails due to the hardware, i.e. memory, limit, CBE-TDVP fails due to diverging SVD during the shrewd selection process. This is still an advantage given we have an efficient algorithm to fix this problem.

Table 4: Running time for the TDVP methods for the SB model

g	Method	Without noise		With noise	
		Time (s)	Average Bond Dim	Time (s)	Average Bond Dim
0.01	CBE-TDVP	107.85	11.5	113.97	11.5
	TDVP2	258.16	5.5	278.43	6
0.1	CBE-TDVP	110.30	11.5	137.89	11.5
	TDVP2	619.46	7	961.32	8.5
1	CBE-TDVP	180.85	11.5	234.41	11.5
	TDVP2	1521.80	10.75	Hardware limit	
10	CBE-TDVP	279.37	11.25	SVD diverged	
	TDVP2	2152.38	11.5	Hardware limit	
100	CBE-TDVP	SVD diverged		SVD diverged	
	TDVP2	Hardware limit		Hardware limit	

The second observation is that TDVP2 has a mechanism to reduce its bond dimensions as seen more vividly in Figure 3 and 4 while CBE-TDVP doesn't have an explicit way to reduce them. At each iteration, TDVP2 truncates the singular values of the tensors. This enables it to change the bond dimensions according to the singular values. Because CBE-TDVP can only expand the dimensions to a certain maximum, this introduces hyperparameters to be tuned, i.e. finding the most optimal growth and maximum of the dimensions.

After analyzing the speed and the bond dimensions, I tried to fix the cases when the SVD diverged. However, because I couldn't get the corresponding simulation with TDVP2 because of my hardware limit, I decided to present the results using $g = 0.01$ so the results between the two methods can be compared.

On closer inspection, the diverging correlates to the health checks giving non-numerically zero values and approaching 1. One way to bring the health checks closer to 0 is by increasing the SVD's truncation threshold ϵ thereby truncating more singular values. However, this should be avoided because the step should only remove numerically zero singular values.

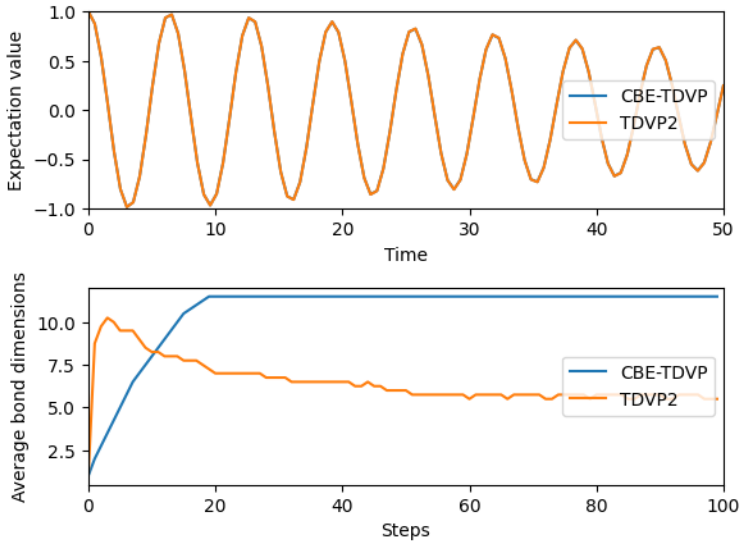

Figure 3: Results using parameters from Table 2 with $g = 0.01$ and without noise

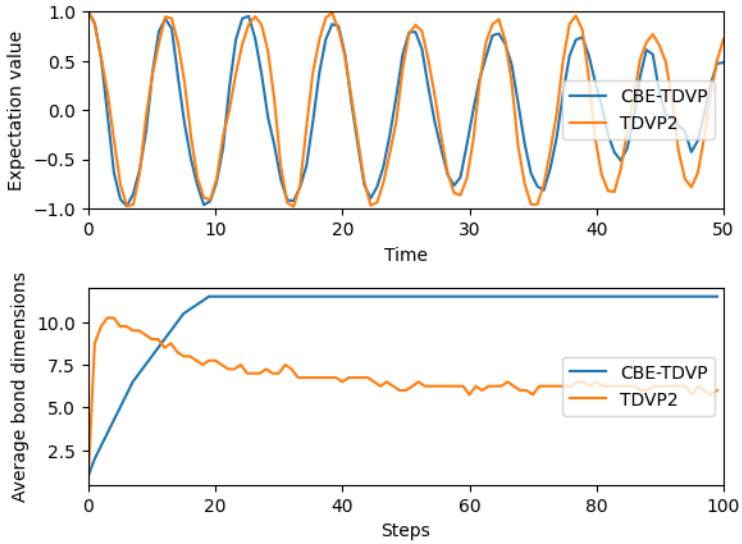

Figure 4: Results using parameters from Table 2 with $g = 0.01$ and noise

As seen in Figure 5, the average bond dimensions stagnate at 7.5 when $\epsilon = 10^{-5}$, below the result from Figure 3 with $\epsilon = 10^{-10}$ which has the average at 11.5. When using $\epsilon = 10^{-5}$ and $\epsilon = 10^{-10}$, the bond dimensions are $[2, 8, 12, 8]$ and $[2, 16, 20, 8]$ respectively. This doesn't impact the accuracy in this specific experiment, because the bond dimensions achieved by TDVP2 are still lower than CBE-TDVP. Again, we should limit the bond dimensions only by using $\tilde{D}$ and D_{max} and not by using ϵ.

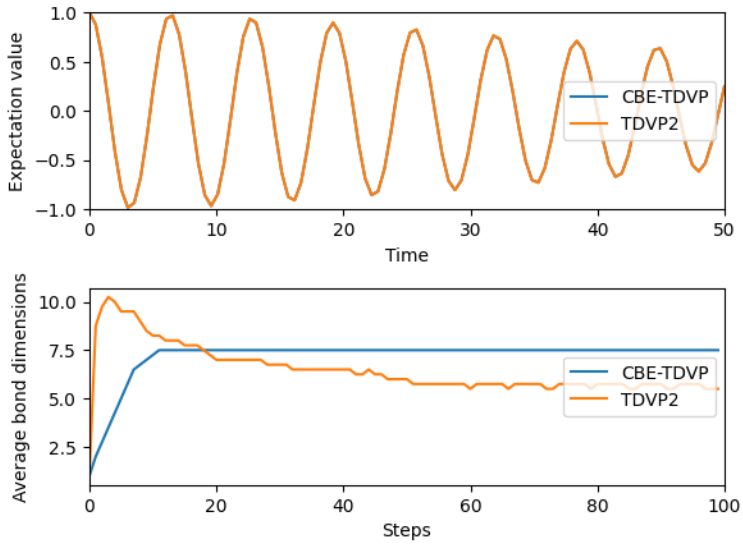

Figure 5: Results using parameters from Table 2 with $g = 0.01$, without noise and $\epsilon = 10^{-5}$

This problem should then be solved by enabling the additional orthogonalization every time the health check gives a value $> 10^{-10}$ and decreasing the truncation threshold from 10^{-10} to 10^{-14}. Figure 6, 7, 8, 9 show the different results with varying truncation thresholds.

For the same threshold of $\epsilon = 10^{-10}$, the one without the additional orthogonalization generates more similar results to TDVP2 results compared with the one with the additional step which can be seen from Figure 4 and Figure 6 respectively. The latter seems to lose some information from the environment resulting in inaccuracies in certain parts.

When the truncation threshold is decreased, the result moves closer to the TDVP2 result. The ideal value is 10^{-14}, as when it gets decreased further, sometimes the new value of the health check after the additional orthogonalization still results in a value in the order of 10^{-1} because we are not truncating the numerically zero values. This method works well with the advantage that adding the step doesn't practically prolong the running time.

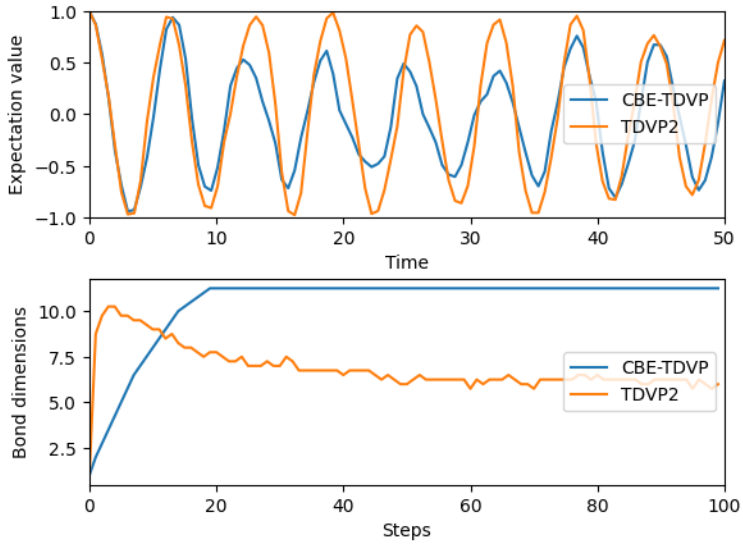

Figure 6: Results from Table 2 with additional orthogonalization and $\epsilon = 10^{-10}$

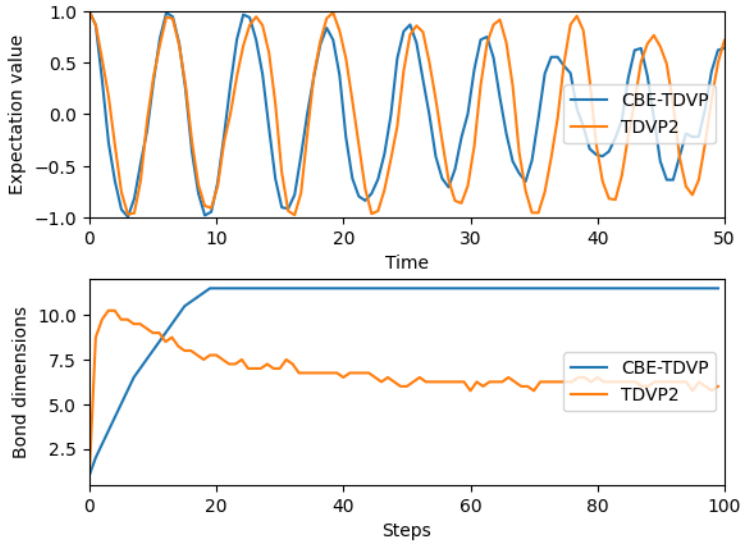

Figure 7: Results from Table 2 with additional orthogonalization and $\epsilon = 10^{-13}$

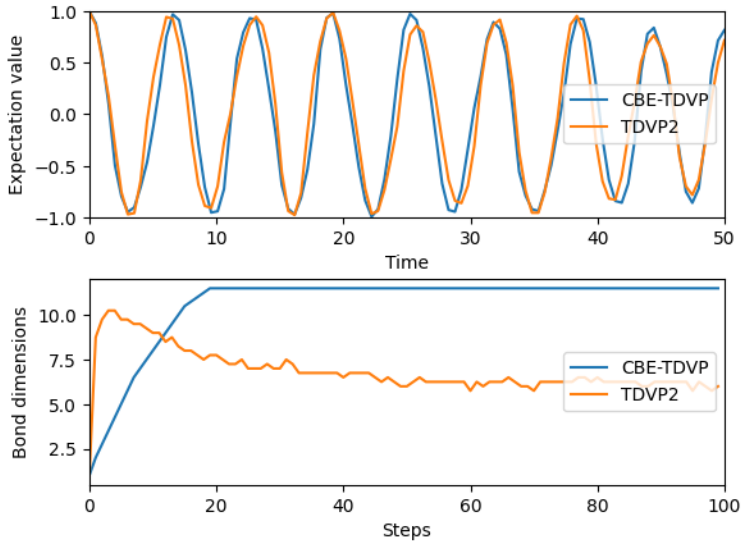

Figure 8: Results from Table 2 with additional orthogonalization and $\epsilon = 10^{-14}$

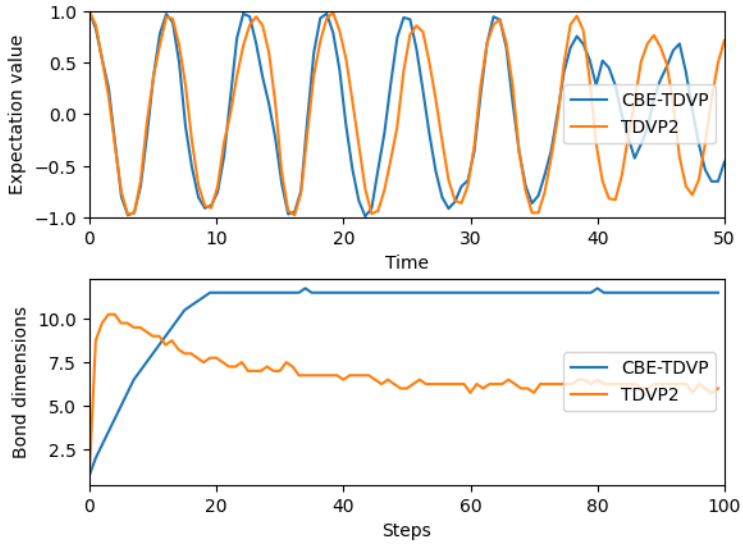

Figure 9: Results from Table 2 with additional orthogonalization and $\epsilon = 10^{-15}$

6. Conclusions and further research

CBE-TDVP shows an important benefit compared to TDVP1 and TDVP2 methods. Especially in an open quantum system where the bond dimensions play an important role in the relationship between the system and the environment, CBE-TDVP can help speed up the simulations by almost a factor of 10 or more in some experiments.

There are some precautions however when using CBE-TDVP. First, there are more hyperparameters to tune compared to both TDVP1 and TDVP2 and those are the truncation threshold ϵ, the maximum bond dimension D_{max}, and the truncated complement dimension $\tilde{D}$. Finding the optimal parameters might lead us to use more time than simulating with TDVP2.

The behaviour of the health checks and the orthogonalization still need to be researched further for more complicated models. There might be some use cases where CBE-TDVP doesn't work or the extra orthogonalization doesn't give better results. We must test the limitations of this method and improve the method accordingly.

References

[1] J. Roden, W. T. Strunz, and A. Eisfeld, "Non-Markovian quantum state diffusion for absorption spectra of molecular aggregates", *J. Chem. Phys.* **134**, 034902 (2011).

[2] A. Di Paolo, T.E. Baker, A. Foley, D. Sénéchal, and A. Blais, "Efficient modeling of superconducting quantum circuits with tensor networks", *npj Quantum Inf.* **7**, 11 (2021).

[3] C.J. Wood, J.D. Biamonte, and D.G. Cory, "Tensor networks and graphical calculus for open quantum systems," *Quant. Inf. Comput.* **15**, 759 (2015).

[4] J. Haegeman, J.I. Cirac, T.J. Osborne, I. Pižorn, H. Verschelde, and F. Verstraete, "Time-dependent variational principle for quantum lattices," *Phys. Rev. Lett.* **107**, 070601 (2011).

[5] D. Suess, A. Eisfeld, and W.T. Strunz, "Hierarchy of stochastic pure states for open quantum system dynamics," *Phys. Rev. Lett.* **113**, 150403 (2014).

[6] L. Chen, D. I. G. Bennett, A. Eisfeld, "Simulation of absorption spectra of molecular aggregates: A hierarchy of stochastic pure state approach," *J. Chem. Phys.* **156**, 124109 (2022).

[7] X. Gao, J. Ren, A. Eisfeld, and Z. Shuai, "Non-Markovian stochastic Schrödinger equation: Matrix-product-state approach to the hierarchy of pure states," *Phys. Rev. A* **105**, L030202 (2022).

[8] J.-W. Li, A. Gleis, and J. von Delft, "Time-dependent variational principle with controlled bond expansion for matrix product states," 2022, *arxiv:2208.10972*.

[9] J. Haegeman, C. Lubich, I. Oseledets, B. Vandereycken, and F. Verstraete, "Unifying time evolution and optimization with matrix product states," *Phys. Rev. B* **94**, 165116 (2016).

[10] A. Gleis, J.-W. Li, and J. von Delft, "Controlled bond expansion for DMRG ground state search at single-site costs," *Phys. Rev. Lett.* **130**, 246402 (2023).

[11] B. Sappler, "Benchmarking a tensor network algorithm for the HOPS-method to simulate open non-markovian quantum systems," B.S. thesis, School of Comput. Inform. and Technol., Tech. Univ. of Munich, Munich, 2023.